A Bogus Typhoon Scheme and Its Application to a Movable Nested Mesh Model

Wang Guomin (王国民)
Department of Atmospheric Sciences, Nanjing University, Nanjing 210093
Wang Shiwen (王诗文) and *Li Jianjun* (李建军)
National Meteorological Center, China Meteorological Adminstration, Beijing 100081
Received November 21, 1994; revised June 26, 1995

ABSTRACT

A bogus typhoon scheme, designed for the initialization of a typhoon track prediction model, is developed in this paper. This scheme includes both effects of axisymmetric wind and asymmetric wind. Experimental forecasts using a two-way interactive movable nested mesh model show that the forecast skill of typhoon tracks has clearly improved after introducing the bogus typhoon into the initial fields.

Key words: Bogus typhoon, Track forecast, Nested mesh model

I. INTRODUCTION

The gale and the heavy rainfall caused by typhoons are one of the major natural disasters that influence the coastal areas of China, so typhoon forecasting (primarily the typhoon track forecasting nowadays) is very important both theoretically and practically. Because typhoons form and develop over oceanic regions where conventional synoptic observations are sparse and are not well reliable, typhoon track forecasting is often failure by using a numerical model initialized from the assimilation of a large-scale model. On the other hand, computers of today are capable of running high-resolution primitive equation numerical prediction models operationally. Therefore, in order to perform the numerical prediction of typhoon tracks, we must enhance the information that could represent a typhoon as realistic as possible in observed analysis fields. A common way is, based upon a set of observational parameters, to construct a semi-empirical model typhoon (usually called as a bogus typhoon), and then to implant the bogus typhoon into the analyzed field. In this way some experimental forecasts of typhoon tracks have shown encouraging results, examples have included the works of Iwasaki et al. (1987), Mathur (1991) and Kurihara et al. (1993).

Following the above works, we present here a bogus typhoon scheme. It includes both an axisymmetric typhoon structure and an asymmetric wind structure related to the axisymmetric one. Prediction experiments using a movable nested mesh model show that this scheme is feasible.

II. OUTLINES OF THE NESTED MESH MODEL

A primitive equation model and σ (in the vertical) and latitude-longitude (in the horizontal) coordinate system are adopted. It is formulated in 15 levels and C-type staggering grid mesh. The model physics includes horizontal diffusion, surface boundary friction, large-scale precipitation and cumulus parameterization (for details see National Meteorological Center, 1990). Time integration uses an economical explicit scheme (Tatsumi, 1983).

The coarse mesh model (CM) is fixed with a horizontal resolution 1.875°, and a model domain covering the area of 0–48.75°N, 84.375–159.375°E, which consists of 27 × 41 grid points. The CM lateral boundary is updated by using a technique suggested by Davis (1976). The fine mesh model (FM) follows the movement of a typhoon, with a resolution of 0.46875° and a domain size of 18.75° × 18.75° or 41 × 41 grid points. So the ratio of grid lengths of CM to FM is 4:1. The vertical structures are identical for both CM and FM.

Time integrations proceed with CM fields firstly. The latest tendency, $\Delta X = X^{n+1} - X^n$ of CM variable X, is obtained after completion of one step integration from time steps n to $n+1$. The CM tendency, ΔX, is spatially and temporally interpolated to get time-dependent FM tendency that is used to update the FM lateral boundary. Then the FM integrates four successive time steps (here assuming that the ratio of time steps of CM to FM is also 4:1) until reaching the time level same as that of the CM. At this time level the forecasted CM fields are superseded by the smoothing values of the latest FM forecasts over the FM domain where FM fields overlap with CM ones, this means that a feedback of FM to CM is performed. The smoothing is a nine-point spatial filter. After above steps one cycle of integrations of the nested mesh model is completed. From the above procedure, the updating of FM boundary by the CM forecast result implies the forcing of large-scale motions on the FM fields, and the feedback of the FM forecasts to the CM ones represents the influences of a typhoon on large-scale flow. For those who want other details about the nested mesh model, please refer to Wang et al. (1995).

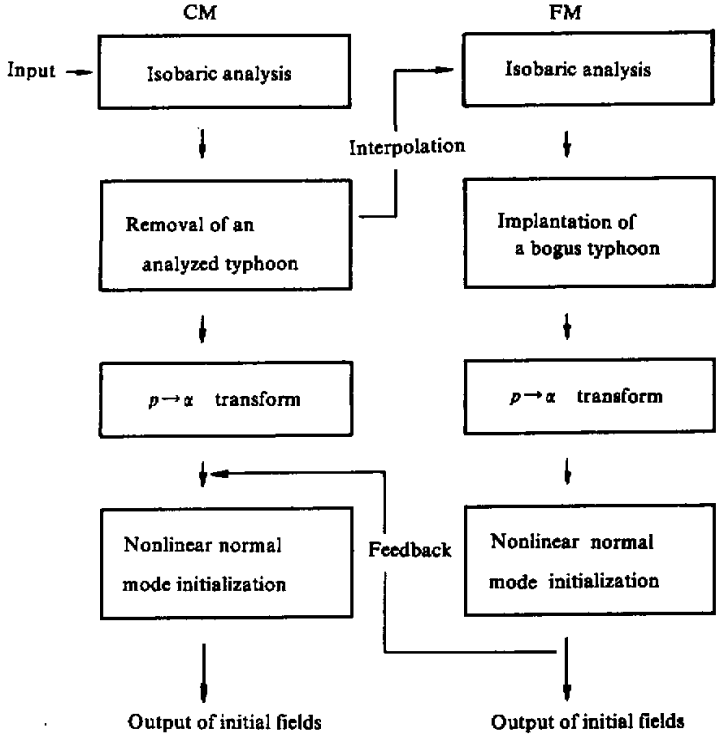

Fig. 1. Flow diagram of initialization processes for the nested model.

The initialization processes of the nested model is given in Fig.1. The bogus typhoon is added to the interpolated FM isobaric analysis fields. After the initialized FM have been formed, the feedback operation as used in the forecast model is applied in order to introduce the bogus typhoon information into the CM model.

III. BOGUS TYPHOON SCHEME

1. *Removal of an Analyzed Typhoon*

A typhoon existing in the large–scale analysis field is usually a weak vortex, its intensity and location differ much from those of the real situation. Before implanting the bogus typhoon we have to remove this unrealistic weak vortex (hereafter called as analyzed typhoon). The approach to remove an analyzed typhoon is the two–step filterings proposed by Kurihara et al. (1993). Zonal and meridional filterings are first applied to analysis field to isolate an analyzed typhoon from the disturbance field. An operation of subtracting an analyzed typhoon from analysis field results in the large–scale environmental field. As seen from Fig. 1 this operation is carried out in the CM mesh domain.

Zonal direction filtering is a local three–point smoothing operator given by

$$h_{J,I} = h_{J,I} + \alpha(h_{J,I-1} + h_{J,I+1} - 2h_{J,I}) \ , \tag{1}$$

where h is an arbitrary scalar variable, subscripts (J,I) refer to the meridional and zonal indices respectively, and α is the filtering parameter defined as

$$\alpha = \frac{1}{2}\left(1 - \cos\frac{2\pi}{m}\right)^{-1} \ . \tag{2}$$

To eliminate waves with wave length less than 9°, Eq.(1) is performed successively for $m = 2,3,4,5$ in Eq.(2). After the completion of filtering in the zonal direction, a similar filtering is applied in the meridional direction, that is,

$$\bar{\bar{h}}_{J,I} = \bar{h}_{J,I} + \alpha(\bar{h}_{J-1,I} + \bar{h}_{J+1,I} - 2\bar{h}_{J,I}) \ . \tag{3}$$

The disturbance field is defined as

$$h_D = h - \bar{\bar{h}} \ . \tag{4}$$

In order to perform a cylindrical filtering we need identifying the center position (λ_0,φ_0) and the radius R_a of an analyzed typhoon. These parameters can be estimated from the 850 hPa disturbance wind speed $V_D = \left(u_D^2 + v_D^2\right)^{1/2}$. The center position is then given by

$$(\lambda_0,\varphi_0) = \frac{\sum(V_D)_{J,I} \cdot (\lambda_{J,I},\varphi_{J,I}) \cdot \Delta S_{J,I}}{\sum(V_D)_{J,I} \cdot \Delta S_{J,I}} \ , \tag{5}$$

where the summation includes those grid points within a 9× 9 CM grid point rectangle subdomain centered at the point nearest to the observed typhoon position (λ_c,φ_c), $\Delta S_{J,I}$ is the area assigned to grid point (J,I), and $(\lambda,\varphi)_{J,I}$ are the grid point longitude and latitude, respectively.

The disturbance field, h_D, then is projected to a polar coordinate system centered at (λ_0,φ_0), and is expressed by $h_D(r,\theta)$, where r is radial distance and θ is azimuth. R_a is now determined from $V_D(r)$, which represents the azimuthal mean of V_D. The $V_D(r)$ increases with radius and reaches maximum at some position. Beyond that position, $V_D(r)$ tends to

monotonically decrease. The first time that the condition of $V_D(r) \leqslant 3\ \mathrm{ms}^{-1}$ is met, that radius is used for R_a. From this point of view, the radius R_a is ensured to enclose the main portion of the analyzed typhoon.

Having known λ_0, φ_0 and R_a, the analyzed typhoon h_a is obtained through a cylindrical fillter:

$$h_a(r,\theta) = [1 - E(r)][h_D(r,\theta) - \bar{h}_D(R_a)] \ , \tag{6}$$

where $\bar{h}_D(R_a)$ is the azimuthal average of h_D at radius R_a. The cylindrical filter function takes the form:

$$E(r) = \frac{\exp[-(R_a - r)^2 / l^2] - \exp(-R_a^2 / l^2)}{1 - \exp(-R_a^2 / l^2)} \ , \tag{7}$$

where l is a parameter controlling the $E(r)$ shape, and here is set to $R_a / 5$.

The analyzed typhoon so obtained is near axisymmetric, its strength decreases gradually outwards from the center, and vanishes at $r = R_a$. The large-scale environmental field, h_E, is then defined by subtracting the analyzed typhoon from the original analysis field:

$$h_E = h - h_a \ . \tag{8}$$

After completing the above processes of obtaining h_a, the h_E field would vary continuously and smoothly over the area of an analyzed typhoon.

2. *Axisymmetric Typhoon*

In the polar coordinate system centered at the location of the observed typhoon, based on the observed typhoon's central pressure p_c, the pressure of the outermost closed isobar p_b and the corresponding radius R_b (see Appendix for the estimates of p_b and R_b), an empirical formula is used to generate the axisymmetric profile of the surface pressure:

$$p_s(r) = \begin{cases} p_m - [\Delta p \cdot \exp(-x^2)] / (1 + ax^2)^{1/2} \ , & r \leqslant R_b \\ p_b \ , & r > R_b \end{cases} \tag{9}$$

where r is radius distance, $x = r / R_b$, a is parameter controlling the location of maximum cyclonic winds and is set to 100, the constants p_m and Δp can be evaluated from the conditions $p_s(0) = p_c$ and $p_s(R_b) = p_b$.

The surface pressure, through an empirical relation (see Appendix (A2)), is used to obtain the geopotential height at 1000 hPa:

$$\Phi_s(r) = 8.8g(p_s(r) - 1000) \ , \tag{10}$$

where g is the acceleration due to gravity. From the gradient wind equation:

$$V^2 / r + f_0 V - \partial\Phi / \partial r = 0 \ , \tag{11}$$

the wind at 1000 hPa, $V_s(r)$, can be obtained within $r \leqslant R_b$. Here f_0 is the Coriolis parameter at the position of the typhoon center.

Set the wind to be zero at $r = R_a$, the wind within the zone of $R_b < r < R_a$ is evaluated by assuming that the wind decreases linearly from $V_s(R_b)$ at $r = R_b$ to $V_s(R_a) = 0$ at $r = R_a$. To eliminate weak discontinuity, a fifth order polynomial fit is applied to the symmetric flow defined within $r \leqslant R_a$. The tangential wind thus obtained is used to derive an asymmetric flow (see next subsection). After this step the target tangential wind at

1000 hPa, $V_t(r,1000)$, is determined.

Introducing the empirically determined structure functions:

$$F(p)=\frac{1}{2}[1+\tanh\left(\pi\frac{p-p'}{\Delta p}\right)]\ , \tag{12a}$$

$$G(p)=\operatorname{sech}\left(\frac{p-p'}{\Delta p}\right)\ , \tag{12b}$$

$$H(r)=\operatorname{sech}\left(\frac{r-r'}{\Delta r}\right)\ , \tag{12c}$$

the winds on the other mandatory levels are given by

$$V_t(r,p)=[F(p)-G(p)H(r)]\cdot V_t(r,1000)\ . \tag{13}$$

The parameters p', Δp, r' and Δr in (12) control the decreasing rate of cyclonic winds in the vertical and the height of anticyclonic winds in the upper level, and they are set to 150 hPa, 200 hPa, 280 km and 200 km, respectively.

Set the geopotential height to be zero at $r=R_a$, the axisymmetric deviations of geopotential on each level, $\Delta\Phi(r,p)$ can be evaluated also by use of the gradient wind equation from the above obtained target tangential wind.

The moisture field related to the bogus typhoon is estimated by a very simple way. Let the relative humidity (RH) deviation at 1000 hPa be

$$\Delta H(r,1000)=\Delta H_c\cdot\left(1-\frac{r}{R_a}\right)\ . \tag{14}$$

The ΔH on the other levels is given by

$$\Delta H(r,p)=\{\sin[(\frac{p-p_t}{1000-p_t}\frac{\pi}{2}]\}\cdot\Delta H(r,1000)\ , \tag{15}$$

where ΔH_c is set to 8%, and p_t is 300 hPa. Since the RH is about 90% over the coverage of a typhoon and surroundings in the lower troposphere, the RH in bogus typhoon is specified to be about 98% near the lower level central region.

3. *Introduction of Asymmetric Winds*

Dynamical analysis on typhoon motions has shown that, in the absence of basic flow, the typhoon's motion is almost caused by the nonlinear interactions of the symmetric flow and the β effect, this kind of movement is usually termed as β drift (Smith and Ulrich, 1990). In performing typhoon track predictions by a dynamical model, the β drift mechanism will be an important factor that could improve the track forecast skills. It is apparent especially when the environmental steering flow is very weak. Kurihara et al. (1993) have made an interesting attempt to include the effects of asymmetric winds associated with the β drift by using a simplified barotropic model and have given encouraging results. Guided by their work, we introduce here the asymmetric winds into the symmetric bogus typhoon described in the previous subsection.

According to Ross and Kurihara(1992), the wavenumber–one structure around the typhoon is the predominant part of the asymmetric winds related to the β drift, they could be accurately simulated by a three–component barotropic vorticity equation model. In other words, the total wind can be decomposed in a polar coordinate system moving with the ty-

phoon center as

$$\vec{V}(r,\theta) = \vec{V}_0(r) + \vec{V}_1(r,\theta) + \vec{V}_2(r,\theta) \ , \tag{16}$$

or the vorticity field is expressed as

$$\zeta(r,\theta) = \zeta_0(r) + \zeta_1(r,\theta) + \zeta_2(r,\theta) \ , \tag{17}$$

where the subscript denotes the azimuthal wavenumber, with the wavenumber 0 being the symmetric component. Set the β drift velocity at the typhoon center to be $\vec{C}$, the governing equations for the components can be deduced from the bartropic vorticity equation as

$$\frac{\partial \zeta_0}{\partial t} = -(\vec{V}_1 \cdot \nabla\zeta_1)_0 - (\vec{V}_2 \cdot \nabla\zeta_2)_0 + (\vec{C} \cdot \nabla\zeta_1)_0 - \beta(\vec{j} \cdot \vec{V}_1)_0 \ , \tag{18}$$

$$\frac{\partial \zeta_1}{\partial t} = -\vec{V}_0 \cdot \nabla\zeta_1 - \vec{V}_1 \cdot \nabla\zeta_0 - (\vec{V}_1 \cdot \nabla\zeta_2)_1 - (\vec{V}_2 \cdot \nabla\zeta_1) \ ,$$
$$+ \vec{C} \cdot \nabla\zeta_0 + (\vec{C} \cdot \nabla\zeta_2)_1 - \beta\vec{j} \cdot \vec{V}_0 - \beta(\vec{j} \cdot \vec{V}_2)_1 \ , \tag{19}$$

$$\frac{\partial \zeta_2}{\partial t} = -\vec{V}_0 \cdot \nabla\zeta_2 - \vec{V}_2 \cdot \nabla\zeta_0 - (\vec{V}_1 \cdot \nabla\zeta_1)_2 + (\vec{C} \cdot \nabla\zeta_1)_2 - \beta(\vec{j} \cdot \vec{V}_1)_2 \ , \tag{20}$$

where $(\vec{A} \cdot \vec{B})_n$ is the wavenumber n component resulting from the inner product of vectors $\vec{A}$ and $\vec{B}$, and $\vec{j}$ is the unit vector pointing to the north. Given an initial symmetric wind $\vec{V}_0(r)$, Eqs.(18)–(20) can be solved numerically with estimating the radial derivative by finite differencing. We take the tangential wind $\vec{V}_s(r)$ in the previous subsection as $V_0(r)$. The integration shows that, in general, the asymmetric flow becomes fully developed in about 20 hours. However an extended integration to 36 hours has been conducted to reach a quasi–steady state of the asymmetric flow that could be assumed as a representative of a real typhoon asymmetric flow. Such assuming may be reasonable for cases of mature and steady typhoon, but further considerations are necessary for those typhoons in developing, decaying or intensity sharp changing stages.

It is shown from Eq.(18) that the development of asymmetric flow could influence the initial symmetric flow as well, however this influence is not significant. Stated as above, the revised symmetric wind is taken as the $V_t(r,1000)$ in Eq.(13).

The generated surface asymmetric flow is distributed vertically to upper levels by an empirical method. Because there is no practical understanding of the realistic vertical structure of asymmetric flow, we have simply assumed here, as proposed by Kurihara et al. (1993), that the strength of the asymmetric winds decreases monotonically with the height:

$$\vec{V}_a(r,\theta,1000) = \vec{V}_1(r,\theta,1000) + \vec{V}_2(r,\theta,1000) \ ,$$
$$\vec{V}_a(r,\theta,p) = \gamma(p) \cdot \vec{V}_a(r,\theta,1000) \ , \tag{21}$$

where $\gamma(p)$ is the coefficient with the numerical values given in Table 1.

Table 1. Numerical Values for Coefficients $\gamma(p)$.

p (hPa)	850	700	500	400	≤ 300	
$\gamma(p)$	1.0	0.95	0.85	0.5	0.0	if p_c < 990 hPa
	1.0	0.90	0.60	0.0	0.0	if $p_c \geq$ 990 hPa

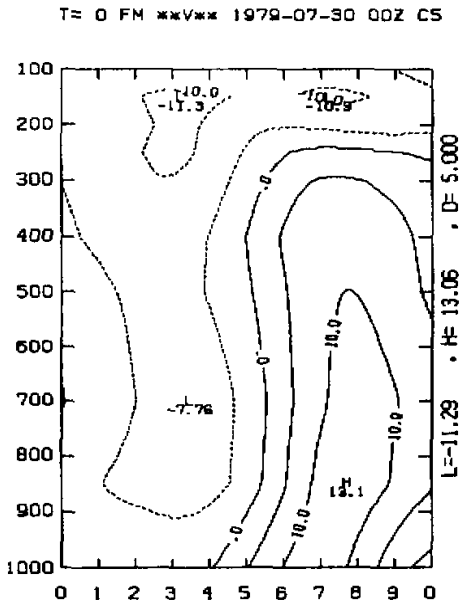

Fig. 2. Pressure–longitude cross section nearest the typhoon center for analyzed meridional wind, the contour interval is 5 ms^{-1}, abscissa is in longitude with interval of 1.875°, vertical coordinate is in hPa.

4. *Discussion*

It is shown by the above processes that only three parameters (longitude, latitude of typhoon center and central pressure) are needed to generate a bogus typhoon by this sheme. It alleviates somewhat the subjective determining of parameters. Moreover, for the bogus typhoon is implanted, as the form of a deviation field, in the environmental field with an analyzed typhoon excluded, the initial positioning error of an analyzed typhoon is removed as well.

From (9) we see that the p_c has a direct impact on the strength of the symmetric flow. Because an intense typhoon cannot be prescribed well with the models, the p_c is set to 975 hPa whenever a p_c less than 975 hPa is observed. Though this process usually results in a weakening of a typhoon, the study by DeMaria (1985) has shown that, in concerning the movement of a typhoon, the size is more important than the strength of a typhoon.

IV. EXAMPLES

Six case experiments have been conducted for typhoon Judy, Tip and Hope of year 1979 by using the bogus typhoon scheme described previously. Among the above six cases, three of them started from 0000 UTC 23 August, 0000 UTC 11 November and 0000 UTC 30 July, respectively, and another three started just one day later than the former three cases correspondently. The observed tracks of these three typhoons were in directions of northwestward to northeastward, westward, and northwestward, respectively. Here only one case results of 30 July are given in detail.

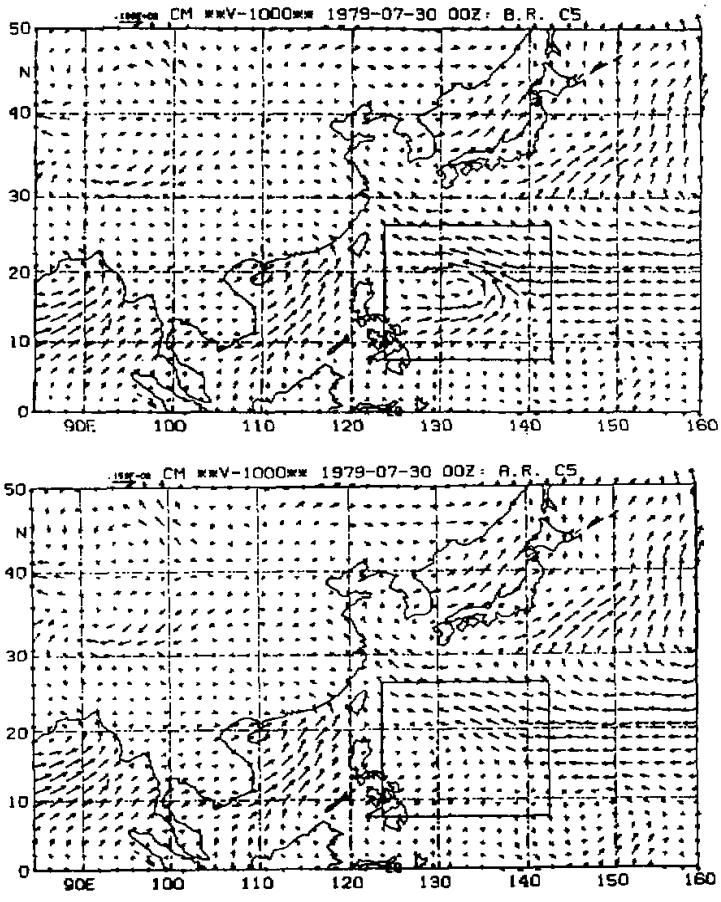

Fig. 3. Winds at 1000 hPa; (a) analyzed, (b) same as (a) but with the analyzed typhoon removed (Ra = 1000 km). The line frame within the figure domain represents the FM boundaries at the initial time.

From the best estimates for typhoon Hope, the central position is at $\lambda_c = 133.5°$E, $\varphi_c = 17.0°$N, central pressure is 955 hPa and maximum wind is 40 ms^{-1} at 0000 UTC 30 July. Fig. 2 shows the analyzed meridional wind near the typhoon center on pressure–longitude cross section. The intensity and strength of the typhoon based on analysis, as seen from the figure, are much weaker than those of the observed typhoon which can be inferred from parameters given in the best estimates. The analysis winds at 1000 hPa is displayed in Fig. 3a, and the corresponding wind fields with the analyzed typhoon removed (Ra = 1000 km) is shown in Fig. 3b. Comparing these two figures, we see that the analyzed typhoon has been effectively filtered out. The same is true for other fields (figures not shown).

With 975 hPa as p_c input value, the scheme generates an initialized state with estimated $p_b = 1007.1$ hPa, $R_b = 648$ km. Fig. 4 shows the pressure–longitude cross section of the initialized meridional wind and Fig. 5 shows the wavenumber–1 asymmetric wind field.

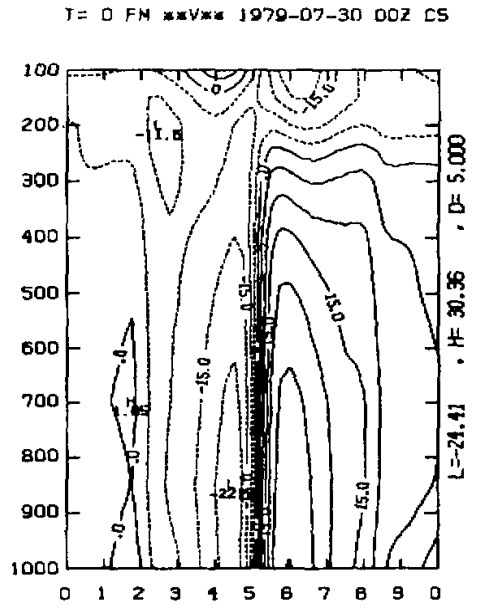

Fig. 4. Pressure–longitude cross section nearest the typhoon center for the initialized meridional wind, the contour interval is 5 ms^{-1}, abscissa is in longitude with interval of 1.875°, vertical coordinate is in hPa.

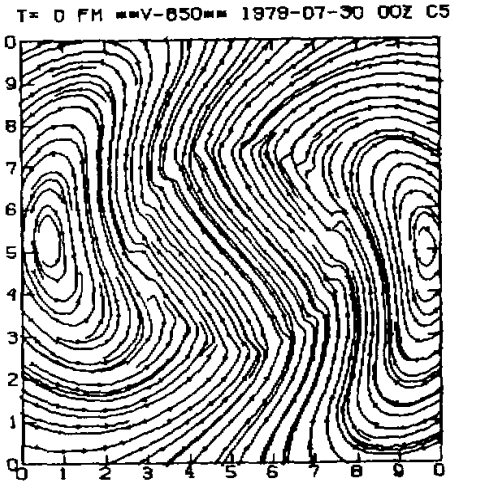

Fig. 5. Streamlines of wavenumber–one asymmetric wind at 850 hPa. Abscissa is in longitude and ordinate is in latitude with intervals of 1.875°.

Forced by the initial symmetric wind, the asymmetric wind develops progressively. It is seen from Fig. 5 that, up to 36h, a uniform flow with the velocity speed of 3.2 ms^{-1} and the direc-

tion of 316°over the typhoon central area, and a dipole–like pattern with an anticyclonic gyre to the east and a cyclonic gyre to the west 900 km far from the center, are formed.

The combination of the symmetric and asymmetric winds leads to an asymmetry in the initialized tangential winds at middle and lower levels, in other words, the south wind in the east side is stronger than the north wind in the west side of the typhoon center, which can be seen in Fig. 4. In addition, we see that there exists an anticyclonic circulation at and above 200 hPa level. Fig. 6 shows the initialized CM wind at 1000 hPa. Compared with Fig. 3a, the main advantages of bogus typhoon are in intensification and improvement of typhoon structures over the typhoon area. Also we notice that the winds vary smoothly across the model inner boundaries. The thermal dynamical fields match well each other with a warm core observed around the typhoon center (figure not shown). Therefore the bogus typhoon structures generated by this scheme in general agree with the observational typhoon structures. Using the initialized fields, the track predictions performed by a two–way movable nested mesh model are shown in Fig. 7. The track errors at 24h and 48h are 58 km 170 km, respectively.

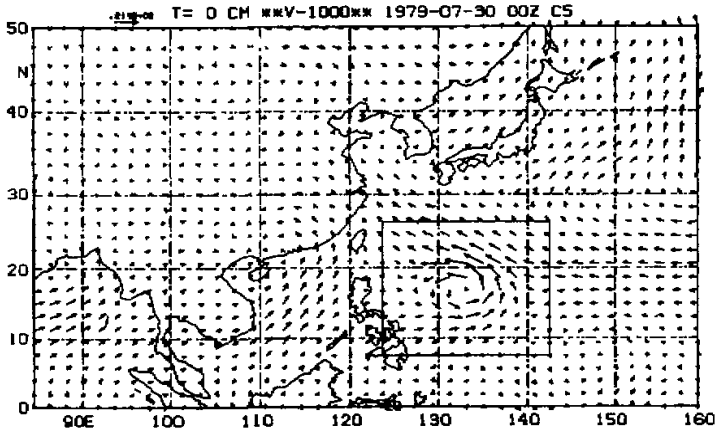

Fig. 6. Initialized wind at 1000 hPa. The line frame within the figure domain denotes the FM boundaries at the initial time.

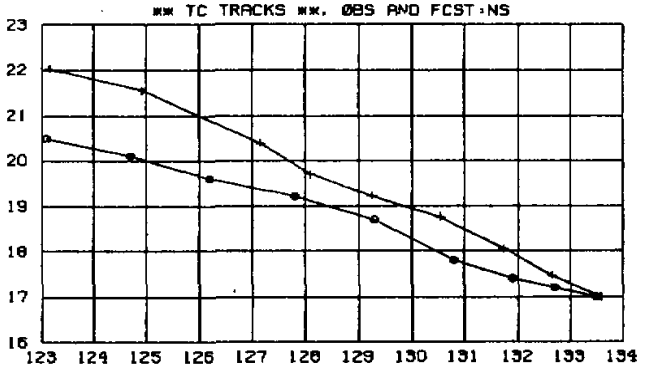

Fig. 7. Observed versus forecasted typhoon tracks. Symbol o represents observed positions, symbol + denotes forecasted positions. The time interval between symbols is 6h. Numerals along abscissa and ordinate stand for longitude and latitude, respectively.

Experimental forecasts are also conducted for other five cases. It is shown that the mean track errors for all six cases at 24h and 48h are 125 km and 382 km, respectively, which demonstrates some forecast skills.

V. DISCUSSIONS

1. *Comparison with Analyzed Initialization*

The cases used here are taken from FGGE dataset, it means that the resolution and quality in the analysis are well-conditioned. Nevertheless, the track prediction performed by the same model but directly using the analysis as initial fields, for example the 30 July case, showed that the track errors at initial time and at 12h are 98 km and 269 km, respectively, after that the track errors increase slowly but the typhoon moves disorderly. This demonstrates that the direct use of the analysis as initial data is inappropriate.

2. *Comparison with Symmetric Flow Initialization*

To investigate the effect of asymmetric winds on the initialization in the bogus typhoon scheme, additional experiments are also conducted in which no asymmetric flow is included. It is shown that when the typhoon locates near the edge of a subtropical high (a case of clear steering current), the effect of asymmetric flow is not important; when the typhoon is far from the subtropical high or the high is weak (cases of weak steering currents), the inclusion of asymmetric winds could improve the prediction skill of typhoon tracks. These results probably indicate that the dynamical mechanism related to the asymmetric flow within a typhoon is responsible for the improvement in the forecase skill of typhoon tracks when the steering current is weak. However, how this mechanism works is not clearly known, and a series of specifically designed prediction experiments should be conducted so as to confirm the roles played by the inner mechanism associated with the typhoon's asymmetric flow.

VI. CONCLUSION

A new bogus typhoon scheme is proposed in this paper. This scheme is based on the syntheses of a few other typhoon initialization schemes. A detailed description of the scheme as well as the case experimental predictions are given. The main conclusions are as follows.

(1). According to this scheme only three parameters (central longitude and latitude, and central pressure of a typhoon) are needed for the system to automatically generate a bogus typhoon, few parameters are specified subjectively.

(2). In the bogus typhoon scheme an asymmetric flow effect is introduced. This asymmetric flow is derived from a simplified model through the forcing of a target symmetric winds. Experimental results show that the introduction of asymmetric flow could improve the forecast skill of typhoon tracks.

(3). Because the bogus typhoon is added, as a deviation field, to the environmental field from which a poor resolved analyzed typhoon is removed, this scheme automatically removes the initial positioning errors of the analyzed typhoon as well.

(4). Results of six case experimental forecasts up to 48h indicate that this bogus typhoon scheme is applicable.

Although the performance of the model using the initial conditions generated by the bogus typhoon scheme has been satisfactory in the cases tested so far, prediction experiments under the operational environments are needed in order to improve further the present scheme. Moreover, studies on exploring the mechanism, to which the forecast skill improve-

ment in typhoon tracks could be attributed by introducing the asymmetric flow into the initial conditions, are also necessary.

Appendix: Estimation of p_b and R_b

The analysis datasets used here do not include the sea level pressure p_{sl}, but contain the geopotential at 1000 hPa, Z_{1000}. An empirical relation is adopted to obtain p_{sl} from Z_{1000}:

$$p_{sl} = Z_{1000} / 8.8 + 1000 , \tag{A1}$$

The p_b, as indicated by Mathur (1991), is the pressure of the outermost closed isobar around a typhoon, R_b is the corresponding radius. To avoid subjective determination of p_b and R_b, the automated estimations of p_b and R_b from Z_{1000} are used.

In a polar coordinate system (r,θ) centered at the minimum of Z_{1000} in FM domain, the azimuthal average of Z_{1000} is expressed as $Z_s(r)$. At point (r,θ), the maximum difference between Z_{1000} and $Z_s(r)$ is $\Delta Z_{\max}(r)$. If the Z_{1000} were an ideal symmetric field, then the $\Delta Z_{\max}(r)$ would be zero everywhere. In general the $\Delta Z_{\max}(r)$ is a monotone increasing function of r. Setting ΔZ_c to be a critical value, a condition of $\Delta Z_{\max}(r) \geq \Delta Z_c$ means that the quasi-axisymmetry of a typhoon is no longer sustained (or an isobar is not closed). The minimum radius that meets the condition is defined as R_b. Then from (A1) p_b can be evaluated as

$$p_b = Z_s(R_b) / 8.8 + 1000 . \tag{A2}$$

The test results show that, when ΔZ_c is set to 25 m, the values of p_b and R_b by the automated estimation and by a subjective evaluation are very close to each other.

REFERENCES

Davis, H. C. (1976), A lateral boundary formulation for multi-level prediction model, *Quart. J. Roy. Meteor. Soc.*, **102**: 405–418.

DeMaria, M. (1985), Tropical cyclone motion in a nondivergent barotropic model, *Mon. Wea. Rev.*, **113**: 1199–1210.

Iwasaki, T., H. Nakano and M. Sugi (1987), The performance of a typhoon track prediction model, *J. Meteor. Soc. Japan*, **65**: 555–570.

Kurihara, Y., M. A. Bender and R. J. Ross (1993), An initialization scheme of hurricane models by vortex specification, *Mon. Wea. Rev.*, **121**: 2030–2045.

Mathur, M. B. (1991), The National Meteorological Center's quasi Lagrangian model for hurricane prediction, *Mon. Wea. Rev.*, **119**: 1419–1447.

National Meteorological Center (1990), Middle-range numerical weather prediction and the product application, Vol. 1. (in Chinese).

Tatsumi, Y. (1983), An economical explicit time integration scheme for a primitive model, *J. Meteor. Soc. Japan*, **61**: 269–287.

Ross, R. J. and Y. Kurihara (1992), A simplified scheme to simulate asymmetries due to the beta effect in barotropic vortices, *J. Atmos. Sci.*, **49**: 1620–1628.

Smith, R. K. and W. Ulrich (1990), An analytical theory of tropical cyclone motion using a barotropic model, *J. Atmos. Sci.*, **47**: 1973–1986.

Wang G., S. Wang and S. Ma (1995), A two-way movable nesting procedure for a typhoon track prediction model (to be published).